

# Cluster spin glass in a chromium-iron system

V. I. Goman'kov, A. I. Zaitsev, I. M. Puzei, and B. N. Tret'yakov

*I. P. Bardin Research Institute of Ferrous Metallurgy*

(Submitted 19 January 1988)

Zh. Eksp. Teor. Fiz. **94**, 292–297 (July 1988)

The changes of the magnetic states have been determined in a system undergoing a spinodal decay upon annealing near the concentration antiferro-ferromagnetic transitions. Annealing leads to in formation of clusters enriched with iron atoms that influence the magnetic correlation-parameters; this causes a shift of the critical concentrations, a rise of the Néel and Curie temperatures, and changes in the spin-glass freezing temperatures. A correlation is established between the dimensions of the magnetic clusters and the changes of the freezing temperature; this makes it possible to identify the spin glass in the Cr-Fe system as being of the cluster type.

## 1. INTRODUCTION

Spin glass is formed in a Cr-Fe solid-solution system near the critical iron concentration  $C_0 = 19$  at. % of the concentration antiferro-ferromagnetic transitions.<sup>1</sup> It is assumed here that the ferromagnetic order sets in via growth of ferromagnetically bound magnetic clusters of nearest-neighbor Fe atoms. At the same time, when the system is annealed below 823 K, a spinodal decay is observed<sup>2</sup> to concentration regions that are richer and poorer in Fe atoms. One expects therefore in the system a tendency to atomic clustering that alters the magnetic state of the alloys. It is therefore proposed that a correlation exists between the atomic and magnetic clustering<sup>3</sup> and influences the spin-glass formation.

We report here the results of direct investigations of decay processes and of magnetic states in annealed alloys; this makes it possible to establish the atomic and magnetic correlations and determine the form of the spin glass. The investigations were carried out by neutron-diffraction and magnetic methods.<sup>4</sup> The magnetic and structural states of quenched and annealed alloys were investigated in a concentration range  $5\% < C_{Fe} < 28\%$ . To stimulate the spinodal decay, the samples were annealed at 773 K, with the annealing durations decreased from 300 to 30 h for compositions of the chosen concentration interval

## 2. RESULTS OF EXPERIMENTS

*Antiferromagnetic and structural states.* Long-range antiferromagnetic order is observed in all quenched and annealed samples for  $C_{Fe} < 16\%$ . Figure 1a shows parts of neutron-diffraction patterns of the alloys near the critical concentration  $C_0$ . Similar neutron-diffraction patterns were obtained for all antiferromagnetic alloys. In a quenched alloy with  $C_{Fe} = 18\%$  there was observed a short-range antiferromagnetic order (Fig. 1a) that is not changed noticeably by annealing for 50 h. Alloys with  $C_{Fe} = 13$  and 15% reveal, after annealing, an increase of the Néel temperature  $T_N$  determined from the temperature dependences of the peak intensity of the (100) antiferromagnetic reflection (Fig. 1b). For compositions with  $C_{Fe} < 10\%$ , the change of  $T_N$  after annealing does not exceed the measurement errors, and the values of  $T_N$  themselves agree with the data of Ref. 5 for quenched alloys (see Fig. 6a).

Besides the rise of  $T_N$ , annealing is observed to be followed by nuclear small-angle neutron scattering (SNS)

which attests to a spinodal decay in the alloys.<sup>2</sup> Figure 2 shows the angular dependences of the intensities of the nuclear SNS, obtained at 300 K. They show that the Fe-atom-enriched regions that result from the annealing are coherently related. Calculation of the correlation function, which is the averaged self-convolution of the particle density,<sup>6</sup>

$$\gamma(r) = \frac{1}{2\pi^2} \int_0^\infty I_n(q) \frac{\sin qr}{qr} q^2 dq,$$

( $r$  is the running coordinate and  $I_n$  is the intensity of the nuclear SNS) and of the distribution function in distance

$$P(r) = r^2 \gamma(r)$$

makes it possible to determine their inertia radius  $R_g$  and diameter for these regions. It follows from Fig. 2b that within the limits of error the value of  $R_g$  hardly increases with increase of  $C_{Fe}$ . The values of  $R_g$  and of the diameter of the regions are, in the spherical approximation,  $8.0 \pm 1 \text{ \AA}$  and  $22.5 \pm 2.5 \text{ \AA}$ , respectively. The maximum of the function  $P(r)$  increases with increase of  $C_{Fe}$  in the alloy, evidencing that the concentration of the Fe atoms increases in the Guin-

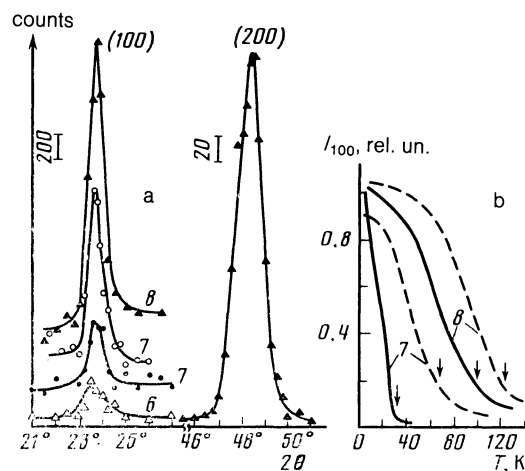


FIG. 1. a—Parts of neutron diffraction patterns ( $\lambda = 1.19 \text{ \AA}$ ) of alloys with different values of  $C_{Fe}$  at 4.2 K; 6—18%; 7—15%,  $\circ$ —annealing,  $\bullet$ —quenching; 8—13% (here and below the numbers on the curves correspond to the numbers of samples with different compositions) b—temperature dependences of peak intensity of (100) antiferromagnetic reflection: solid curves—quenching, dashed—annealing; arrows— $T_N$ .

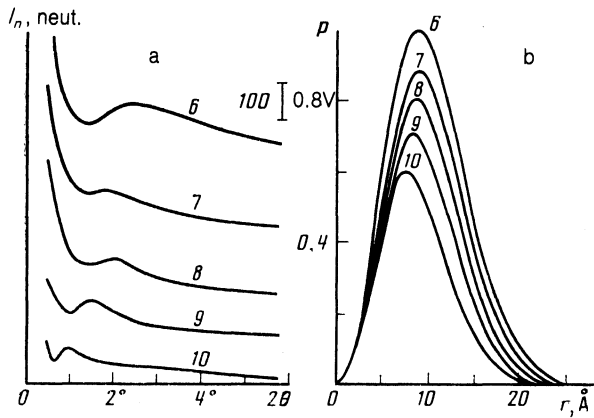


FIG. 2. Angular dependences of the intensities of nuclear SNS at  $\lambda = 1.94 \text{ \AA}$  (a) and the distribution functions in distance for the regions in annealed alloys (b) with different values of  $C_{\text{Fe}}$ : 6—18%; 7—15%; 8—13%; 9—10%; 10—6.8%.

ier-Preston zones. The inertia-radius and diameter values obtained for the regions agree with the reciprocal  $1/k$  of the nuclear correlation parameter calculated from the equation

$$I_n \approx A / (k^2 + q^2), \quad q = 4\pi\lambda^{-1} \sin \theta,$$

where  $A$  is the amplitude,  $\theta$  the scattering angle, and  $\lambda$  the neutron wavelength. In turn, the average distances  $d$  between the regions, estimated from the maxima of the curves of Fig. 2a, decrease smoothly with increase of  $C_{\text{Fe}}$ , from 110  $\text{\AA}$  for  $C_{\text{Fe}} = 6.8\%$  to 50  $\text{\AA}$  for  $C_{\text{Fe}} = 18.0\%$ . This decrease of  $d$  and the corresponding increase of the number of regions, on the one hand, and the loss of iron from the matrix, on the other, lead to an increase of  $T_N$  upon annealing at  $C_{\text{Fe}} > 10\%$  (Fig. 6a).

Together with the atomic clustering upon annealing, a growth of the magnetic clustering is observed; in studies of magnetic SNS this growth is seen even in quenched alloys.<sup>1,7</sup>

Figure 3 shows the temperature dependences of the intensity  $I_m$  of magnetic SNS at  $q = 0.0375 \text{ \AA}^{-1}$  for several quenched and annealed antiferromagnetic as well as ferromagnetic alloys. It can be seen that the value of  $I_m$  at 4.2 K is

is larger for the antiferromagnetic annealed alloy 7 than the value of  $I_m$  for a quenched alloy. This increase of  $I_m$  is observed for all annealed antiferromagnetic alloys, thus attesting to enhancement of the magnetic inhomogeneity upon annealing. The obtained reciprocals  $1/\kappa$  of the magnetic-correlation parameters at 4.2 K also increase after annealing in the case of antiferromagnetic alloys (see Fig. 6b). This increase of the sizes of the magnetic-correlation regions is apparently due to the increase of the Fe content in regions produced as a result of spinodal decay. Thus, the observed growth of  $T_N$  after annealing is connected with the "elimination" of the  $T_N$ -lowering Fe atoms from the antiferromagnetic matrix.

*Long-range ferromagnetic order and spin glass.* In the ferromagnetic composition region ( $C_{\text{Fe}} \geq 19\%$ ) one observes after annealing a rise of the Curie temperatures  $T_C$ . The rise of  $T_C$  is demonstrated in Fig. 3 for the alloy 5. Similar curves were obtained for all the ferromagnetic compositions. This effect is confirmed by measurements of the temperature dependences, shown in Fig. 4, of the differential magnetic susceptibility  $\chi_{ac}$ . The broadening of curves 3–6 for ferromagnetic alloys after annealing attests both to an increase of  $T_C$  and to a decrease of the spin-glass freezing temperatures  $T_g$ . In addition, the values of  $\chi_{ac}$  do not vanish at 4.2 K, indicating the presence of residual magnetization.

The increase of  $T_C$  after annealing (see Fig. 6) is due to enrichment of the ferromagnetic region with iron atoms, as follows also from Fig. 2b. Thus, the increase of  $T_C$  after annealing leads to a shift, in concentration, of the start of formation of the long-range magnetic order. The shift of the peak  $I_0$ —of the intensity of the critical concentrational magnetic SNS—after annealing is demonstrated in Fig. 5. It can be seen that in annealed alloys the antiferro-ferromagnetic transition is effected at lower values of  $C_{\text{Fe}}$ . The values of  $\kappa$  obtained for 4.2 K (see Fig. 6b) also point to a shift of  $C_0$  towards lower values of  $C_{\text{Fe}}$ .

The onset of long-range ferromagnetic order on annealing is demonstrated by curves 6 of Fig. 3. In the quenched

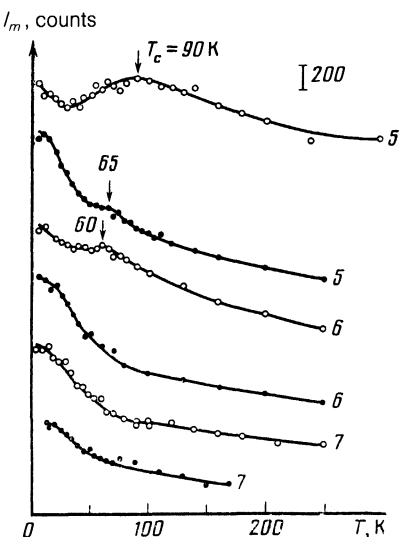


FIG. 3. Temperature dependences of the intensities of magnetic SNS at  $q = 0.0375 \text{ \AA}^{-1}$ : ●—quenching, ○—annealing.

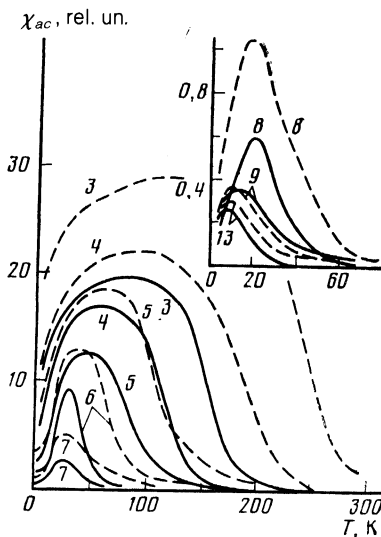


FIG. 4. Temperature dependences of the differential magnetic susceptibility of alloys for different values of  $C_{\text{Fe}}$ : 3—24%; 4—22%; 5—20%; 6—18%; 7—15%; 8—13%; 9—10%; 13—8.5%. Solid curves—quenching, dashed—annealing.

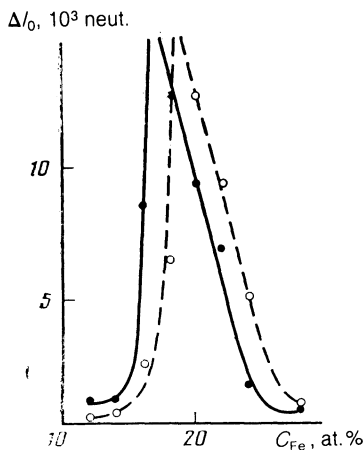


FIG. 5. Concentration dependence of the intensity of magnetic SNS at  $T = 5$  K,  $q = 0$ ; ●—quenching, ○—annealing.

state of this alloy, only spin glass is observed (Fig. 4). Upon annealing the average size of the ferromagnetic clusters reaches  $\sim 60$  Å and long-range order sets in (see Fig. 6a).

The values of  $T_g$  were determined from the temperature dependences of  $\chi_{ac}$  (Fig. 4), and good agreement with the results of Refs. 1 and 7 is observed for quenched alloys. In annealed alloys, a change takes place in the values of  $T_g$ , which attests to the influence of the spinodal decay on the spin glass. The values of  $T_g$  increase in antiferromagnetic alloys and decrease in ferromagnetic ones.

### 3. MAGNETIC-STATE DIAGRAMS AND CONCENTRATIONAL ANTIFERRO-FERROMAGNETIC TRANSITION

The obtained values of  $T_N$ ,  $T_C$ , and  $T_g$  of quenched and annealed alloys were used to plot the magnetic-state diagrams shown in Fig. 6a. The diagram of the quenched alloys agrees in general with the data of Refs. 1 and 7. Since long-range antiferromagnetic order has been observed at 4.2 K, there exists in the region  $8\% < C_{Fe} < 16\%$  below the  $T_g$  limit a two-phase magnetic state, viz., spin glass and an antiferromagnet. Taking into account the data of Fig. 4 for ferromag-

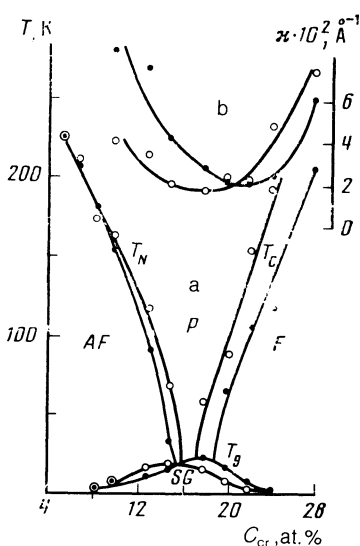


FIG. 6. Magnetic-state diagrams (a) and concentration dependence of magnetic-correlation parameter (b); ●—quenching, ○—annealing.

netic alloys, it can be assumed that the coexistence of the long-range ferromagnetic order with spin glass is preserved at 4.2 K in the region  $17\% < C_{Fe} < 24\%$  below the  $T_g$  boundary.

Figure 6a shows the shift, towards each other, of the long-range-order lines for annealed alloys. It can be assumed that they intersect for longer annealing times. In this case the shape of the diagram is similar to that calculated in Ref. 8. However, the clustering character of the changes of  $T_N$  and  $T_C$ , and apparently of the spin glass itself, leaves the assumed formation of canted structures, of asperomagnetism, and of antiasperomagnetism purely hypothetical.

The increase of  $T_N$  and  $T_g$  after annealing reveals the clustering character of the spin glass in this system. This means that the spin glass is made up of finite ferromagnetic clusters enriched with Fe atoms. On annealing, the average dimensions of the clusters are then increased (Fig. 6b). In antiferromagnetic alloys, the average distance between the clusters also increases, and this in the aggregate raises  $T_g$ . The enlargement of the clusters in ferromagnetic alloys causes the clusters to be attached to a topologically infinite cluster, and hence a lowering of  $T_C$ . There remain finite clusters of smaller size, and this leads to a lowering of  $T_g$ .

These qualitative considerations are confirmed by the correlation between the values of  $\kappa$  and  $T_g$  in Fig. 6. The decrease of the values of  $\kappa$  after annealing of antiferromagnetic alloys is accompanied by a rise of  $T_g$ , whereas an increase of  $\kappa$  after annealing of ferromagnetic alloys corresponds to a lowering of  $T_g$ . It follows directly from this correlation that the spin glass is cluster-like.

### 4. CONCLUSION

Investigation of the Cr-Fe system after annealing has made it possible to establish directly a correlation between atomic and magnetic clustering. One can trace here the magnetic-states variation due to spinodal decay. As expected, the value of  $C_0$  shifts after annealing towards lower values of  $C_{Fe}$ , but the critical concentration at which long-range antiferromagnetic order appears also approaches  $C_0$ . It is assumed that they intersect and long-range orders coexist with spin glass at 4.2 K.

The correlation of the quantities  $\kappa$  and  $T_g$ , observed after annealing the alloys, is a direct confirmation of the clustering of spin glass. The obtained coherence of atomic clusters enriched with Fe atoms after annealing is evidence of interaction of these clusters. In this case the theoretical model of interacting clusters<sup>9</sup> is perfectly applicable to a description of spin glass in Cr-Fe systems.

<sup>1</sup>S. K. Burke, R. Cywinski, J. A. Davis, and B. D. Rainford, *J. Phys.* **F13**, 451 (1983).

<sup>2</sup>E. Z. Vintaikin, V. Yu. Kolontsov, and É. A. Medvedev, *Izv. AN SSSR, Metall.*, No. 4, 169 (1969).

<sup>3</sup>F. Kajzar, G. Parette, and B. Babic, *J. Phys. Chem. Sol.* **42**, 501 (1981).

<sup>4</sup>V. I. Goman'kov, B. N. Tretyakov, and V. I. Kleinerman, *Zh. Eksp. Teor. Fiz.* **88**, 1827 (1985) [*Sov. Phys. JETP* **61**, 1083 (1985)].

<sup>5</sup>S. K. Burke and B. D. Rainford, *J. Phys.* **F8**, 1239 (1978).

<sup>6</sup>D. I. Svergun and L. A. Feigin, *X-ray and Neutron Small-Angle Scattering* [in Russian], Nauka, p. 40.

<sup>7</sup>Yu. A. Dorofeev, A. Z. Men'shikov, and G. A. Takzei, *Fiz. Metall. Metalloved.* **55**, 948 (1983).

<sup>8</sup>M. V. Medvedev and A. V. Zaborov, *ibid.* **52**, 472 (1981).

<sup>9</sup>A. I. Mitsek, *Fiz. Tverd. Tela (Leningrad)* **26**, 2311 (1984) [*Sov. Phys. Solid State* **26**, 1402 (1984)].

Translated by J. G. Adashko